

# Reviews

## Property Degradation of Tetragonal Zirconia Induced by Low-Temperature Defect Reaction with Water Molecules

Xin Guo<sup>†</sup>

*Elektrokeramische Materialien, Institut für Festkörperforschung, Forschungszentrum Jülich, 52425 Jülich, Germany*

*Received April 6, 2004. Revised Manuscript Received June 23, 2004*

Tetragonal ZrO<sub>2</sub> exhibits good ionic conductivity, high strength, and fracture toughness. But while annealing at relatively low temperatures (63–400 °C), tetragonal ZrO<sub>2</sub> spontaneously transforms to a monoclinic one, and its electrical and mechanical properties degrade severely. The phenomenological observations of the low-temperature degradation of tetragonal ZrO<sub>2</sub> are summarized, and major degradation mechanisms are critically reviewed. It is crucial to maintain sufficient oxygen vacancy concentration to stabilize the tetragonal structure; excess reduction of the oxygen vacancy concentration causes the tetragonal to monoclinic transformation. Water molecules can be incorporated into the ZrO<sub>2</sub> lattice by filling oxygen vacancies, which leads to the formation of proton defects. Experimental and theoretical evidence support such a defect reaction between oxygen vacancies and water molecules. And a degradation mechanism based on this defect reaction satisfactorily explains all the phenomenological observations. The diffusion rate of oxygen vacancies at low temperatures is not high enough to cause the observed degradation depth; therefore, the relatively fast diffusion of proton defects most probably controls the degradation process.

### 1. Introduction

In 1975, Garvie, Hannink, and Pascoe<sup>1</sup> first reported the high strength and excellent fracture toughness of tetragonal ZrO<sub>2</sub>. Later, it is established that the high strength (e.g., 2000 MPa) and toughness (e.g., 12 MPa·m<sup>1/2</sup>) are attributed to the stress-induced martensitic phase transformation of tetragonal phase to a monoclinic one in the vicinity of crack fronts.<sup>2–4</sup> For the first time a ceramic material attains the fracture toughness comparable to steel at room temperature. Tetragonal ZrO<sub>2</sub> has also good ionic conductivity; its conductivity is higher than that of cubic ZrO<sub>2</sub> at temperatures <700 °C.<sup>5</sup> However, there exists a major drawback for tetragonal ZrO<sub>2</sub> ceramic: tetragonal ZrO<sub>2</sub> undergoes a spontaneous tetragonal to monoclinic transformation in the presence of water or water vapor when annealed at relatively low temperatures (63–400 °C), engendering cracks in the transformed surface due to the volume expansion accompanying the phase transformation, thereby severely degrading the electrical and mechanical properties.<sup>6–110</sup> This phenomenon is called “low-temperature degradation of tetragonal ZrO<sub>2</sub>”. The catastrophic consequence is shown in Figure 1 in which a tetragonal ZrO<sub>2</sub> sample crumbled to small debris after annealing in 26 mbar water vapor at 250 °C for 30 days.

It is striking that a ceramic pellet disintegrated to isolated grains (Figure 1c).

The first report of the low-temperature degradation of tetragonal ZrO<sub>2</sub> was made by Kobayashi, Kuwajima, and Masaki<sup>6</sup> in 1981. Since then, much research has been performed on the degradation and majority of the works are given in refs 7–110 in chronological order. The degradation has not yet been fully understood, although many degradation mechanisms have been proposed. In this article the advantages and disadvantages of typical degradation mechanisms are elaborated, with an objective of determining the most appropriate degradation mechanism.

### 2. Phenomenological Observations of the Degradation

Although the works on the low-temperature degradation are not totally in accord with each other, the following features of the degradation have been generally accepted:

(1) The tetragonal to monoclinic transformation proceeds from the surface to the interior.<sup>6–110</sup> A diffusion process controls the transformation as indicated in Figure 2. The volume expansion accompanying the phase transformation cracks ZrO<sub>2</sub> samples, and the cracking is intergranular (see, e.g., Figure 1c).<sup>10,49,90,109</sup>

(2) The degradation occurs at relatively low temperatures (e.g., 63–400 °C<sup>10,14,24,27–29,34,36,41,45,52,53,56,61,84</sup>),

<sup>†</sup> Tel: +49-2461-616147. Fax: +49-2461-612550. E-mails: x.guo@fz-juelich.de; guo@IWE.RWTH-Aachen.de.

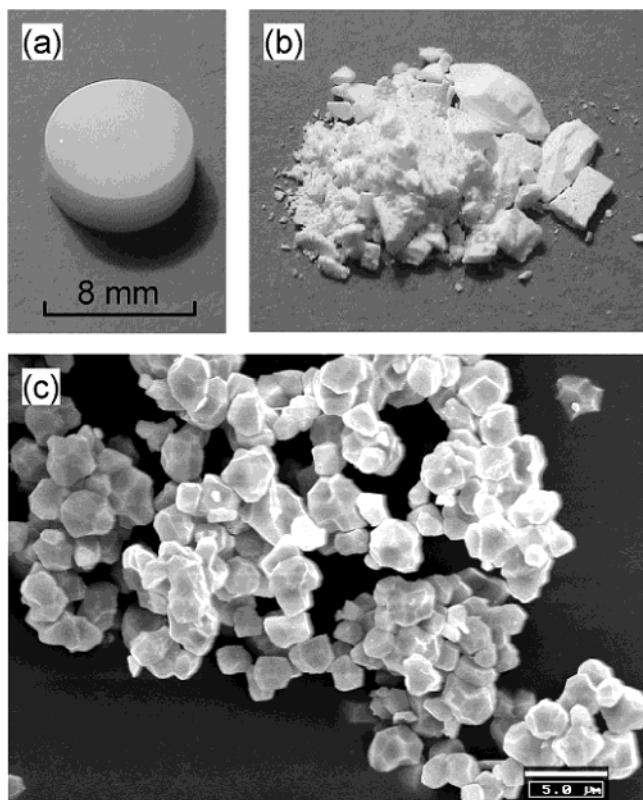


**Figure 1.** 3 mol %  $\text{Y}_2\text{O}_3$ -doped  $\text{ZrO}_2$  ceramic sample at different stages: (a) as-sintered, (b) after annealing in 26 mbar water vapor at 250 °C for 30 days, and (c) scanning electron micrograph of fractured debris.

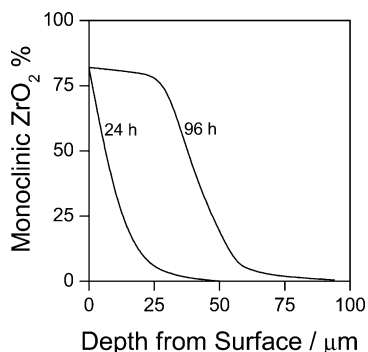


**Figure 2.** Transformation depth profile in 2 mol %  $\text{Y}_2\text{O}_3$ -doped  $\text{ZrO}_2$  after annealing at 300 °C in air for 24 and 96 h, respectively (after Iio et al.<sup>22</sup>).

and at temperatures around 250 °C the degradation is most pronounced.<sup>8,19,23,27–29,50,56,57</sup>

(3) Of all the major constituents of air, only water vapor causes the tetragonal to monoclinic transformation.<sup>7,18,22,65</sup> The degradation rate increases with increasing water vapor pressure,<sup>24</sup> and the degradation becomes much more severe in the presence of water.<sup>11,17,21,24,29,34,61,62,71</sup> The acidic or basic addition in aqueous solution does not have a noticeable influence on the formation of monoclinic  $\text{ZrO}_2$ .<sup>10,11</sup>

(4) The degradation is more marked in the case of lower dopant content (see, e.g., Figure 3).<sup>13,14,19–21,23,27,29,34,79</sup>

(5) Decreasing grain size retards the degradation.<sup>9,13,14,18,19,21,23,25,27–30,34,61,102,108,110</sup> When the tetragonal grain size is below a critical value, the degradation is significantly retarded. The critical grain size is dopant level dependent; e.g., the critical grain size increases

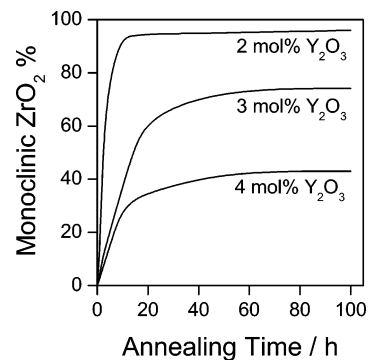


**Figure 3.** Time dependence of monoclinic  $\text{ZrO}_2$  percentage in the surface layers of 2, 3, and 4 mol %  $\text{Y}_2\text{O}_3$ -doped  $\text{ZrO}_2$  samples while annealed at 200 °C in 15.4 mbar water vapor (after Sato et al.<sup>24</sup>).

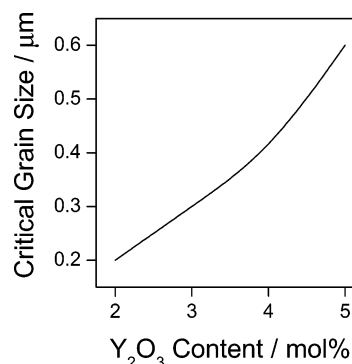


**Figure 4.** Critical tetragonal grain size as a function of  $\text{Y}_2\text{O}_3$  content (after Watanabe et al.<sup>9</sup>). The samples with an average grain size below the critical grain size did not show any sign of degradation after annealing at 300 °C in air for 1000 h.

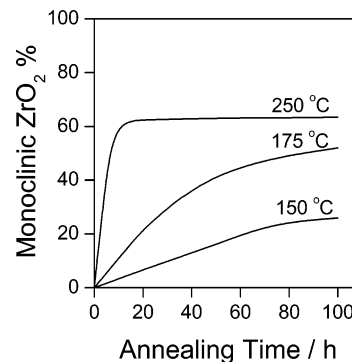


**Figure 5.** Time dependence of monoclinic  $\text{ZrO}_2$  percentage in the surface layers of 3 mol %  $\text{Y}_2\text{O}_3$ -doped  $\text{ZrO}_2$  samples while annealed in air at 150, 175, and 250 °C, respectively (after Sato et al.<sup>14</sup>).

from 0.2 to 0.6  $\mu\text{m}$  if the  $\text{Y}_2\text{O}_3$  concentration increases from 2 to 5 mol % (Figure 4).

(6) The amount of monoclinic phase increases with annealing time and reaches saturation after annealing for a sufficiently long time (see, e.g., Figure 5).<sup>10,13,14,18,24</sup>

(7) Under certain circumstances the degraded properties can be recovered by annealing at high temperatures in a vacuum or dry atmosphere,<sup>15,27</sup> and the annealing retransforms the monoclinic phase back to the tetragonal phase.<sup>57,65,92</sup>

A viable mechanism should be able to explain the effects of dopant content and grain size and the phenomena of monoclinic phase saturation and retransformation.

### 3. Some Typical Degradation Mechanisms

Many attempts have been taken to explain the degradation; some typical mechanisms are summarized as follows:

**Mechanism by Lange et al.**<sup>18</sup>  $\alpha$ -Y(OH)<sub>3</sub> crystallites (20–50 nm in diameter) were observed in the 6.6 mol % Y<sub>2</sub>O<sub>3</sub>-doped ZrO<sub>2</sub> thin foil with transmission electron microscopy (TEM) after annealing at 250 °C in a water vapor environment for 18 h. Therefore, Lange et al. suggested that water vapor reacted with Y<sub>2</sub>O<sub>3</sub> to form the crystallites and the reaction locally drew Y<sub>2</sub>O<sub>3</sub> from tetragonal grains, transforming the tetragonal grains to monoclinic ones. Winnubst and Burggraaf,<sup>21</sup> Azzoni et al.,<sup>44</sup> and Li et al.<sup>62</sup> supported this mechanism. This mechanism naturally explains the effect of dopant content, and it also explains the effect of critical grain size. Lange et al.<sup>18</sup> pointed out, “as a monoclinic nucleus grows by further diffusion of yttrium, it will achieve a critical size where it can spontaneously grow without further yttrium diffusion to completely transform the tetragonal grain in which it was growing.” If the transformed grain is large enough, microcracking will occur, which provides a path for water to penetrate to another grain, allowing the process to repeat. If the transformed grain is smaller than the critical size required for microcracking, then subsequent transformation will be limited by the long-range diffusion of yttrium ions to the surface. The retransformation can be explained by this mechanism as well. At temperatures higher than 1000 °C the  $\alpha$ -Y(OH)<sub>3</sub> crystallites may react with ZrO<sub>2</sub> and yttrium is redissolved in the grains, which results in a retransformation back to the tetragonal structure. But this mechanism cannot explain the phenomenon of monoclinic phase saturation. In addition, it faces a major challenge: it requires short-range diffusion of yttrium. Yoshimura et al.<sup>27</sup> estimated the diffusion time of yttrium ions over a distance of only 1 nm at 250 °C, which is about 10<sup>29</sup> s. It is very unlikely that the  $\alpha$ -Y(OH)<sub>3</sub> crystallites could be formed by the diffusion of yttrium at 250 °C within only 18 h. And the dissolution of yttrium ions in water has also been disproved by the analysis of the solvent.<sup>11,26,27,92</sup>

**Mechanism by Sato and Shimada.**<sup>11</sup> Water plays an important role in the low-temperature degradation. Therefore, Sato and Shimada proposed the stress corrosion by water; i.e., water reacts with Zr–O–Zr bonds at crack tips and Zr–OH bonds are formed, i.e.,  $-\text{Zr}-\text{O}-\text{Zr}- + \text{H}_2\text{O} \rightarrow -\text{Zr}-\text{OH} + \text{HO}-\text{Zr}-$ . This reaction results in a release of the surface energy that acts to stabilize the tetragonal phase and the growth of pre-existing surface flaws; consequently, the transformation to monoclinic phase proceeds. The compounds with a similar chemical structure to water, e.g., those non-aqueous solvents with a molecular structure containing a lone pair electron orbital opposite a proton donor site, also accelerates the degradation.<sup>11</sup> This mechanism can explain the phenomenon of retransformation. However, Sato and Shimada did not give evidence for the formation of Zr–OH bonds, and how the bond formation causes the release of the surface energy was not explained and proved. More adversely, this mechanism cannot explain the effects of dopant content and grain size and the phenomenon of monoclinic phase saturation.

**Table 1. Lattice Parameters of Monoclinic ZrO<sub>2</sub> Transformed from Tetragonal Phase after Different Treatments<sup>27</sup>**

treatment	<i>a</i> (nm)	<i>b</i> (nm)	<i>c</i> (nm)	$\beta$ (deg)	<i>V</i> (nm <sup>3</sup> )
(1) <sup>a</sup>	0.5165	0.5254	0.5258	98.51	0.1411
(2) <sup>b</sup>	0.5174	0.5252	0.5275	99.06	0.1415
(3) <sup>c</sup>	0.5169	0.5253	0.5266	98.89	0.1413

<sup>a</sup> Mechanical grinding. <sup>b</sup> Annealing in water at 250 °C under 100 MPa for 6 h. <sup>c</sup> Reheating in a vacuum at 400 °C for 6 h.

**Mechanism by Yoshimura et al.**<sup>27,29</sup> Yoshimura et al. demonstrated the introduction of hydroxyl ions OH<sup>−</sup> by low-temperature annealing and the exclusion of OH<sup>−</sup> by reheating in a vacuum or at high temperatures, with subsequent volume change (Table 1) and about 0.233 wt % weight variation. Therefore, they proposed the following degradation mechanism: first step, chemical adsorption of H<sub>2</sub>O on the surface; second step, formation of Zr–OH and/or Y–OH bonds, which brings about the lattice strain on the surface; third step, strain accumulation by the diffusion of OH<sup>−</sup> on the surface and in the lattice; fourth step, the accumulated strain area acts as a nucleus of monoclinic phase in the tetragonal matrix. However, one crucial point of this mechanism, how the formation of Zr–OH and/or Y–OH bonds brings about the lattice strain on the surface and in the bulk, was not explained and proved. This mechanism can explain the effect of dopant content by suggesting the formation of Y–OH bonds and it can also explain the phenomenon of retransformation, but it cannot explain the effect of grain size and the phenomenon of monoclinic phase saturation.

**Mechanism by Hernandez et al.**<sup>36</sup> Hernandez et al. detected hydroxyl ions OH<sup>−</sup> and possibly the formation of Y–OH bonds by means of X-ray photoelectron spectroscopy (XPS). On this basis, they proposed that the degradation occurs by the following steps: (i) adsorption and dissociation of water molecules on the surface, (ii) reaction of OH<sup>−</sup> in the more active points (Y<sub>2</sub>O<sub>3</sub>) to form an oxyhydroxide YO(OH) species that is stable under hydrothermal conditions, (iii) formation of purely tetragonal ZrO<sub>2</sub> embryos which are coherent in the tetragonal matrix, (iv) growth of the embryos to above a critical size and then the tetragonal to monoclinic transformation. It is unclear from ref 36 whether the formation and the growth of purely tetragonal ZrO<sub>2</sub> embryos require the diffusion of cations at low temperatures or not. This mechanism can explain the effect of dopant content by suggesting the formation of YO(OH) species; it can also explain the phenomenon of retransformation but it cannot explain the effect of grain size and the phenomenon of monoclinic phase saturation.

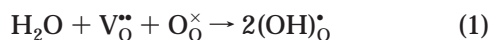
**Mechanism by Kim et al.**<sup>45</sup> Kim et al. detected hydroxyl ions OH<sup>−</sup> after annealing 3 mol % Y<sub>2</sub>O<sub>3</sub>-doped ZrO<sub>2</sub> in water and LiOH solution at 90, 150, and 200 °C. They proposed the following mechanism for the degradation in an aqueous solution: OH<sup>−</sup> ions diffuse through oxygen vacancies and interact with the vacancies to form Zr–OH bonds, which contributes to the tensile strain around the occupied vacancy sites. The buildup of the tensile strain ends up with the onset of the tetragonal to monoclinic transformation. Oxygen vacancies are the most active defects in acceptor-doped ZrO<sub>2</sub>. The merit of this mechanism is that it realizes the importance of oxygen vacancies in the low-temper-

ature degradation. But XPS investigations<sup>30,36,62</sup> indicate the formation of Y–OH bonds, instead of Zr–OH bonds. Yet it is unclear from this mechanism how the tensile strain strong enough to cause the tetragonal to monoclinic transformation is built up. This mechanism can explain the phenomenon of retransformation, but it cannot explain the effects of dopant content and grain size and the phenomenon of monoclinic phase saturation.

#### 4. Point Defects and Low-Temperature Degradation

**4.1. Degradation Mechanism Based on Point Defect Reaction.** Livage et al.<sup>111</sup> suggested that oxygen vacancies play an important role in the stabilization of ZrO<sub>2</sub>. A simulation<sup>112</sup> based on a self-consistent tight-binding model showed that the stabilization of the tetragonal and the cubic structure could be achieved by doping ZrO<sub>2</sub> crystals with oxygen vacancies only. Oxygen vacancies are created in the ZrO<sub>2</sub> lattice by doping with acceptors, e.g., trivalent oxide Y<sub>2</sub>O<sub>3</sub>; however, doping with donors, e.g., pentavalent oxide Nb<sub>2</sub>O<sub>5</sub>, annihilates oxygen vacancies due to the charge compensation Y<sup>3+</sup>/Nb<sup>5+</sup> related to the host Zr<sup>4+</sup>. By creating and annihilating oxygen vacancies in ZrO<sub>2</sub>, Kountourou and Petzow<sup>40</sup> actually proved that there are a critical minimum and a critical maximum oxygen vacancy concentration for the cubic, the tetragonal, and the monoclinic phase, respectively; excess oxygen vacancy concentration variation results in phase transformation. For example, the cubic phase of 8 mol % Y<sub>2</sub>O<sub>3</sub>-doped ZrO<sub>2</sub> was transformed to tetragonal phase by further doping with 6 mol % Nb<sub>2</sub>O<sub>5</sub>;<sup>40</sup> in this case the effective acceptor concentration was equivalent to 2 mol % Y<sub>2</sub>O<sub>3</sub>.

In many oxides, oxygen vacancies can be filled by water molecules according to



where (OH)<sub>O</sub><sup>•</sup> is a proton defect. This reaction is the basis for the proton conduction in, e.g., SrTiO<sub>3</sub>, SrZrO<sub>3</sub>, BaCeO<sub>3</sub>, and Y<sub>2</sub>O<sub>3</sub>.<sup>113–115</sup> Based on this reaction, another mechanism for the low-temperature degradation of tetragonal ZrO<sub>2</sub> has evolved,<sup>72,73,86,89,90,107,109</sup> which consists of the following steps: (i) chemical adsorption of H<sub>2</sub>O on the ZrO<sub>2</sub> surface, (ii) reaction of H<sub>2</sub>O with O<sup>2-</sup> on the ZrO<sub>2</sub> surface to form hydroxyl ions OH<sup>-</sup>, (iii) penetration of OH<sup>-</sup> into the inner part by grain boundary diffusion, (iv) filling of oxygen vacancies by OH<sup>-</sup> ions, and therefore the formation of proton defects, and (v) occurrence of a tetragonal to monoclinic transformation when the oxygen vacancy concentration is reduced to the extent that the tetragonal phase is no longer stable. If the amount of the phase transformation is large enough, due to the volume expansion associated with the phase transformation, both micro- and macro-cracks can be produced in the transformed surface layer, and the cracks open up new surfaces to react with water or water vapor, leading to further spontaneous transformation. As indicated in Figure 2, a diffusion process controls the transformation. This mechanism requires only the diffusion of proton defects.

#### 4.2. Experimental and Theoretical Evidence.

**Formation and Diffusion of Hydroxyl Ions.** Many theo-

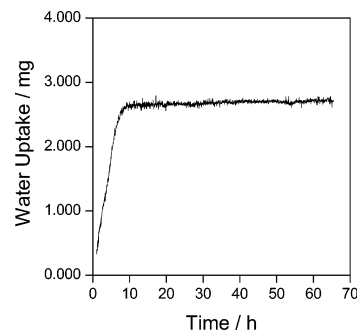


**Figure 6.** Water uptake in 3 mol % Y<sub>2</sub>O<sub>3</sub>-doped ZrO<sub>2</sub> during annealing in 1 bar water vapor at 250 °C (after Guo and Schober<sup>109</sup>).

retical and experimental results support this mechanism. For example, an atomic simulation<sup>116</sup> discloses the dissociative adsorption of water on the tetragonal ZrO<sub>2</sub> surface. And hydroxyl ions (OH<sup>-</sup>) were detected on the tetragonal ZrO<sub>2</sub> surface by X-ray photoelectron spectroscopy (XPS)<sup>30,36,62,73</sup> and infrared adsorption spectroscopy.<sup>27,30,45</sup> A Fourier transform infrared (FT-IR) transmission spectrometry investigation<sup>70</sup> proved that H species penetrated the ZrO<sub>2</sub> bulk after annealing in water. Higher OH<sup>-</sup> concentration was detected by XPS at the grain boundaries of 3 mol % Y<sub>2</sub>O<sub>3</sub>-doped tetragonal ZrO<sub>2</sub> after annealing in boiling water for 40 h,<sup>73</sup> suggesting that OH<sup>-</sup> ions intergranularly diffused into the interior of the sample during annealing. In addition, it was found that the thickness of the degraded layer was strongly related to the diffusion distance of OH<sup>-</sup>.<sup>45</sup> If estimated from Figure 2, the diffusion coefficient of (OH)<sub>O</sub><sup>•</sup> in 2 mol % Y<sub>2</sub>O<sub>3</sub>-doped ZrO<sub>2</sub> at 300 °C is about 3 × 10<sup>-10</sup> cm<sup>2</sup> s<sup>-1</sup>, comparable with that in SrTiO<sub>3</sub> (about 10<sup>-9</sup> cm<sup>2</sup> s<sup>-1</sup> at 300 °C<sup>114,115</sup>). But it is much higher than the diffusion coefficient of oxygen vacancies (about 2 × 10<sup>-14</sup> cm<sup>2</sup> s<sup>-1</sup> in 14.2 mol % CaO-doped ZrO<sub>2</sub> at 300 °C, extrapolated from data between 800 and 1097 °C<sup>117</sup>), suggesting that the diffusion of oxygen vacancies may not be important to the degradation.

**Water Incorporation.** According to the degradation mechanism based on eq 1, steps (i)–(vi) should result in the incorporation of water molecules into tetragonal ZrO<sub>2</sub>. As demonstrated in Figure 6, water was indeed incorporated into 3 mol % Y<sub>2</sub>O<sub>3</sub>-doped ZrO<sub>2</sub> during annealing in 1 bar water vapor at 250 °C.<sup>109</sup> As shown in Figure 6, the water uptake continuously increased within the first ~8 h and then leveled off (or saturated) at ~2.5 mg, corresponding to an incorporation of ~1.5 mol % H<sub>2</sub>O or ~3.0 mol % (OH)<sub>O</sub><sup>•</sup>. A fast process, e.g., grain boundary diffusion, likely accomplished the water incorporation. The phase of the sample was initially totally tetragonal, but after the water incorporation ~73% of the phase became monoclinic. It is noted that the oxygen vacancy concentration in 3 mol % Y<sub>2</sub>O<sub>3</sub>-doped ZrO<sub>2</sub> is 3 mol %. According to eq 1, ~50% of the oxygen vacancies in the sample could be filled by the incorporation of ~1.5 mol % H<sub>2</sub>O; the oxygen vacancy concentration in the sample was then lower than the critical minimum concentration for tetragonal phase (1.7 mol %<sup>40</sup>). Under this condition, the tetragonal phase transformed to the monoclinic one. The incorporation of water molecules into the tetragonal ZrO<sub>2</sub> lattice should cause the lattice expansion; such a lattice expansion was also observed.<sup>109</sup> Yoshimura et al.<sup>27</sup> found that

the volume of the monoclinic structure transformed from the tetragonal phase by annealing in water is larger than that by mechanical grinding (Table 1). This lattice expansion was attributed to the incorporation of OH<sup>-</sup> ions.

**Filling of Oxygen Vacancies by Water Molecules.** Under the condition that oxygen vacancies are totally filled by water molecules,  $[(\text{OH})_0^*]/[\text{V}_0^{**}]$  is expected to be 2 according to eq 1. Here  $[(\text{OH})_0^*]$  is the concentration of the proton defects and  $[\text{V}_0^{**}]$  the initial oxygen vacancy concentration. Kruse et al.<sup>43</sup> annealed 3 mol % Y<sub>2</sub>O<sub>3</sub>-doped ZrO<sub>2</sub> ceramic samples at 200 °C in D<sub>2</sub>O-enriched water vapor with a vapor pressure of 15 bar for 2 h; afterward, they determined the concentration of hydrogen and deuterium by means of elastic recoil detection analysis (ERDA). After the hydrothermal treatment, the combined concentration of hydrogen and deuterium ( $[\text{H}] + [\text{D}]$ ) was about  $1.4 \times 10^{21} \text{ cm}^{-3}$ , whereas the oxygen vacancy concentration,  $[\text{V}_0^{**}]$ , in 3 mol % Y<sub>2</sub>O<sub>3</sub>-doped ZrO<sub>2</sub> is about  $4.33 \times 10^{20} \text{ cm}^{-3}$ . Then  $([\text{H}] + [\text{D}])/[\text{V}_0^{**}] \approx 3$ , comparing with the expected ratio of 2. Within experimental error the agreement is quite good.

**Proton Conduction.** The expected proton conduction was also checked. Water vapor concentration cells,



where one side of a slab of 3 mol % Y<sub>2</sub>O<sub>3</sub>-doped ZrO<sub>2</sub> coated with silver electrodes was exposed to water vapor pressures  $p_{\text{H}_2\text{O}}$  of 30–50 mbar while the other side was constantly held at a  $p_{\text{H}_2\text{O}}$  of 6.1 mbar, were constructed, and the polarity and the Nernst voltage of the cells was checked at 250 °C.<sup>109</sup> The polarity of the observed voltages agreed in all cases with the expected proton conduction. However, there was no clear-cut correlation between the magnitude of the observed Nernst voltages and the partial pressures involved as dictated by Nernst's equation. This failure to yield the expected Nernst voltages is ascribed to the fact that local equilibria were not established near the electrodes. The observed correct polarity, however, is a clear indication that we were dealing with proton conduction in the experiments.

As the mobility of proton defects (OH)<sub>0</sub><sup>\*</sup> is higher,<sup>113–115</sup> it is predicted that the electrical conductivity of the sample should increase by the introduction of proton defects. Attempts<sup>86,90</sup> have been taken to measure the electrical conductivity of 3 mol % Y<sub>2</sub>O<sub>3</sub>-doped tetragonal ZrO<sub>2</sub> while being annealed in water vapor. However, the tetragonal to monoclinic phase transformation and the sample cracking severely affected the sample electrical conductivity; therefore, it is not possible to establish an unambiguous correlation between the conductivity and the proton conduction. However, such a correlation was obtained for 8 mol % Y<sub>2</sub>O<sub>3</sub>-doped cubic ZrO<sub>2</sub>.<sup>107</sup> Cubic ZrO<sub>2</sub> has always been presumed to be stable in the environment known to cause the degradation to tetragonal ZrO<sub>2</sub>. Nevertheless, none of the all above mechanisms prohibits a similar degradation of cubic phase to tetragonal, even to a monoclinic one. For example, the formation of hydroxyl ions on the cubic ZrO<sub>2</sub> surface was also observed by XPS.<sup>89</sup> Recently, similar degradation was also observed

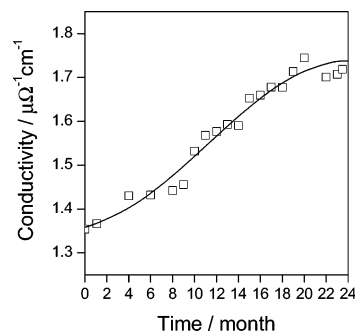


**Figure 7.** Bulk electrical conductivity of 8 mol % Y<sub>2</sub>O<sub>3</sub>-doped ZrO<sub>2</sub> versus annealing time at 250 °C in 26 mbar water vapor (after Guo and He<sup>107</sup>).

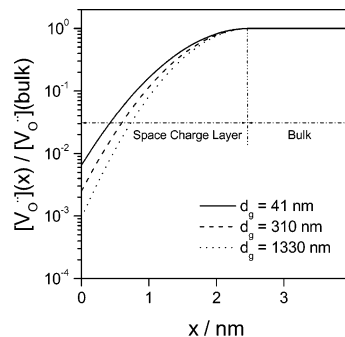


**Figure 8.** Oxygen vacancy profiles in the space charge layers of 3 mol % Y<sub>2</sub>O<sub>3</sub>-doped ZrO<sub>2</sub> samples with different grain sizes ( $d_g$ ) at 550 °C (after Guo and Zhang<sup>124</sup>). In this figure,  $x$  is the distance from the grain boundary,  $[\text{V}_0](x)$  is the oxygen vacancy concentration at  $x$ , and  $[\text{V}_0](\text{bulk})$  the oxygen vacancy concentration in the bulk.

for cubic ZrO<sub>2</sub> (sample cracking and precipitation of monoclinic phase) after annealing in water vapor at 250 °C for 2 years.<sup>107</sup> Unlike tetragonal samples, the degradation only produced a few cracks in the cubic ZrO<sub>2</sub> sample, which makes reliable electrical measurements possible. The bulk electrical conductivity measured by impedance spectroscopy is shown in Figure 7. It has been demonstrated that impedance spectroscopy is an effective technique to monitor in situ the low-temperature degradation.<sup>86,88,90,108,110</sup> As shown in this figure, the bulk conductivity continuously increased with annealing time; about 30% increase was measured, which is attributed to the expected proton conduction. The possibility of proton conduction in ZrO<sub>2</sub> has also been evaluated in refs 118 and 119, in which the experimental evidence supports proton conduction in ZrO<sub>2</sub> in the presence of water vapor. Especially in monoclinic ZrO<sub>2</sub>, proton defects can be significant, while not dominant.<sup>118</sup>

**4.3. Explanation of Phenomenological Observations.** The degradation mechanism based on eq 1 explains the effects of dopant content and grain size and the phenomena of monoclinic phase saturation and retransformation. In the case of high dopant content, more oxygen vacancies should be filled to induce the degradation. The grain boundaries of acceptor-doped ZrO<sub>2</sub> are characterized by a positive grain boundary potential and subsequent depletion of oxygen vacancies in the adjacent space charge layers (Figure 8).<sup>120–124</sup> Such a feature makes the grain boundaries vulnerable to the OH<sup>-</sup> attack, which may explain the intergranular cracking. As demonstrated previously,<sup>123,124</sup> the oxygen vacancy concentration in the space charge layer in-

creases with decreasing grain size (Figure 8). Therefore, more oxygen vacancies in the space charge layer should be filled to induce the degradation at the grain boundaries in the case of finer grain size. Figure 6 is very similar to the plot for 250 °C given in Figure 5, suggesting that the saturation shown in Figure 5 is likely due to the saturation of water incorporation (defined by temperature and water vapor pressure). When heated in a vacuum or to high temperatures, the incorporated proton defects escape from the ZrO<sub>2</sub> lattice, as indicated by the lattice shrinkage shown in Table 1. As a result, reaction 1 is reversed, and then the tetragonal to monoclinic transformation is reversed accordingly.

The majority of the works on the degradation deal with Y<sub>2</sub>O<sub>3</sub>-doped ZrO<sub>2</sub>. However, the modification of the defect structure in ZrO<sub>2</sub> by doping with oxides other than Y<sub>2</sub>O<sub>3</sub>, e.g., MgO, is expected to change the degradation behavior. It has been reported that the degradation of ZrO<sub>2</sub> is retarded by the doping of MgO.<sup>12,20,33,41</sup> Owing to the double charges, magnesium ions (Mg<sub>Zr</sub>'') strongly bind oxygen vacancies (V<sub>O</sub>''), which is evident from the low conductivity of MgO-doped ZrO<sub>2</sub><sup>125</sup> and the very large binding energy of (Mg<sub>Zr</sub>''V<sub>O</sub>''<sup>x</sup>)<sup>x</sup> (-146 kJ/mol, comparing with -39 kJ/mol for (Y<sub>Zr</sub>''V<sub>O</sub>''<sup>126</sup>)). Therefore, the filling of oxygen vacancies by water molecules (eq 1) becomes more difficult; as a result, the degradation of MgO-doped ZrO<sub>2</sub> is retarded. The similar effect of CaO<sup>20</sup> can be similarly explained.

XPS investigations of degraded Y<sub>2</sub>O<sub>3</sub>-doped tetragonal ZrO<sub>2</sub> samples suggested the formation of Y-OH bonds.<sup>36,62</sup> The mechanism based on eq 1 is favorable to the formation of the Y-OH bond because the reaction between proton defects ((OH)<sub>O</sub>') and yttrium ions (Y<sub>Zr</sub>'') is energetically favorable as a result of the opposite charges of the defects. This also helps in explaining the formation of Y(OH)<sub>3</sub> crystallites.

## 5. Concluding Remarks

Similar to the electrical properties, the low-temperature degradation of tetragonal ZrO<sub>2</sub> is dominated by its defect structure. A degradation mechanism based on the point defect reaction between oxygen vacancies and water molecules is developed, which consists of the following steps: (i) chemical adsorption of H<sub>2</sub>O on the ZrO<sub>2</sub> surface, (ii) reaction of H<sub>2</sub>O with O<sup>2-</sup> on the ZrO<sub>2</sub> surface to form hydroxyl ions OH<sup>-</sup>, (iii) penetration of the hydroxyl ions into the inner part by grain boundary diffusion, (vi) filling of oxygen vacancies by the hydroxyl ions, and therefore the formation of proton defects, and (v) occurrence of a tetragonal to monoclinic transformation when the oxygen vacancy concentration is reduced to the extent that the tetragonal phase is no longer stable. The tetragonal to monoclinic transformation may be martensitic, as the martensitic transformation is known under certain circumstances to occur isothermally.<sup>127</sup> This mechanism requires only the diffusion of proton defects at low temperatures, which is a few orders of magnitude higher than that of oxygen vacancies. Comparing with the other ones, this mechanism is soundly supported by theoretical and experimental evidence, and it explains all the phenomenological observations of the low-temperature degradation.

The low-temperature degradation can be retarded by applying one of the following strategies: (1) increase of dopant concentration; (2) reduction of grain size; (3) introduction of inert materials, e.g., CeO<sub>2</sub>,<sup>17,20,36,48,52,56,68,101</sup> TiO<sub>2</sub>,<sup>20,54</sup> Al<sub>2</sub>O<sub>3</sub>,<sup>13,20,35,52,58,63,75,88,93,99,106</sup> CuO,<sup>67,81,100</sup> or carbon;<sup>105</sup> (4) formation of an inert surface layer, e.g., a recrystallized tetragonal layer with finer grain size,<sup>32</sup> or a cubic surface layer,<sup>66</sup> or a silica encapsulating surface layer.<sup>82</sup>

## References

- (1) Garvie, R. C.; Hannink, R. H.; Pascoe, R. T. *Nature* **1975**, *258*, 703.
- (2) Gupta, T. K.; Lange, F. F.; Bechtold, J. H. *J. Mater. Sci.* **1978**, *13*, 1464.
- (3) Porter, D. L.; Evans, A. G.; Heuer, A. H. *Acta Metall.* **1979**, *27*, 1649.
- (4) Evans, A. G.; Burlingame, N.; Drory, M.; Kriven, W. M. *Acta Metall.* **1981**, *29*, 447.
- (5) Weppner, W. *Solid State Ionics* **1992**, *52*, 15.
- (6) Kobayashi, K.; Kuwajima, H.; Masaki, T. *Solid State Ionics* **1981**, *3/4*, 489.
- (7) Murase, Y.; Kato, E. *J. Am. Ceram. Soc.* **1983**, *66*, 196.
- (8) Sato, T.; Shimada, M. *J. Am. Ceram. Soc.* **1984**, *67*, C-212.
- (9) Watanabe, M.; Iio, S.; Fukuura, I. In *Science and Technology of Zirconia II*; Claussen, N., Rühle, M., Heuer, A. H., Eds.; American Ceramic Society: Columbus, OH, 1984; p 391.
- (10) Nakajima, K.; Kobayashi, K.; Murata, Y. In *Science and Technology of Zirconia II*; Claussen, N., Rühle, M., Heuer, A. H., Eds.; American Ceramic Society: Columbus, OH, 1984; p 399.
- (11) Sato, T.; Shimada, M. *J. Am. Ceram. Soc.* **1985**, *68*, 356.
- (12) Swain, M. V. *J. Mater. Sci. Lett.* **1985**, *4*, 848.
- (13) Tsukama, K.; Shimada, M. *J. Mater. Sci. Lett.* **1985**, *4*, 857.
- (14) Sato, T.; Ohtaki, S.; Shimada, M. *J. Mater. Sci.* **1985**, *20*, 1466.
- (15) Matsumoto, R. L. K. *J. Am. Ceram. Soc.* **1985**, *68*, C-213.
- (16) Sato, T.; Ohtaki, S.; Endo, T.; Shimada, M. *J. Am. Ceram. Soc.* **1985**, *68*, C-320.
- (17) Sato, T.; Shimada, M. *Am. Ceram. Soc. Bull.* **1985**, *64*, 1382.
- (18) Lange, F. F.; Dunlop, G. L.; Davis, B. I. *J. Am. Ceram. Soc.* **1986**, *69*, 237.
- (19) Schubert, H.; Petzow, G. In *Science and Technology of Zirconia III*; Sömiya, S., Yamamoto, N., Yanagida, H., Eds.; American Ceramic Society: Westerville, OH, 1986; p 21.
- (20) Sato, T.; Ohtaki, S.; Endo, T.; Shimada, M. In *Science and Technology of Zirconia III*; Sömiya, S., Yamamoto, N., Yanagida, H., Eds.; American Ceramic Society: Westerville, OH, 1986; p 29.
- (21) Winnubst, A. J. A.; Burggraaf, A. J. In *Science and Technology of Zirconia III*; Sömiya, S., Yamamoto, N., Yanagida, H., Eds.; American Ceramic Society: Westerville, OH, 1986; p 39.
- (22) Iio, S.; Watanabe, M.; Kuroda, K.; Saka, H.; Imura, T. In *Science and Technology of Zirconia III*; Sömiya, S., Yamamoto, N., Yanagida, H., Eds.; American Ceramic Society: Westerville, OH, 1986; p 49.
- (23) Hecht, N. L.; Jang, S. D.; McCullum, D. E. In *Science and Technology of Zirconia III*; Sömiya, S., Yamamoto, N., Yanagida, H., Eds.; American Ceramic Society: Westerville, OH, 1986; p 133.
- (24) Sato, T.; Ohtaki, S.; Endo, T.; Shimada, M. In *Science and Technology of Zirconia III*; Sömiya, S., Yamamoto, N., Yanagida, H., Eds.; American Ceramic Society: Westerville, OH, 1986; p 501.
- (25) Arai, T.; Yamamoto, T.; Tsuji, K. In *Science and Technology of Zirconia III*; Sömiya, S., Yamamoto, N., Yanagida, H., Eds.; American Ceramic Society: Westerville, OH, 1986; p 517.
- (26) Yoshimura, M.; Hiuga, T.; Sömiya, S. *J. Am. Ceram. Soc.* **1986**, *69*, 583.
- (27) Yoshimura, M.; Noma, T.; Kawabata, K.; Sömiya, S. *J. Mater. Sci. Lett.* **1987**, *6*, 465.
- (28) Lu, H. Y.; Chen, S. Y. *J. Am. Ceram. Soc.* **1987**, *70*, 537.
- (29) Yoshimura, M. *Am. Ceram. Soc. Bull.* **1988**, *67*, 1950.
- (30) Lepistö, T. T.; Mäntylä, T. A. *Ceram. Eng. Sci. Proc.* **1989**, *10*, 658.
- (31) Chen, S. Y.; Lu, H. Y. *J. Mater. Sci.* **1989**, *24*, 453.
- (32) Whalen, P. J.; Reidinger, F.; Antrim, R. F. *J. Am. Ceram. Soc.* **1989**, *72*, 319.
- (33) Sato, T.; Endo, T.; Shimada, M.; Mitsudome, T.; Otabe, N. *J. Mater. Sci.* **1991**, *26*, 1346.
- (34) Swab, J. J. *J. Mater. Sci.* **1991**, *26*, 6706.
- (35) Tsubakino, H.; Nozato, R.; Hamamoto, M. *J. Am. Ceram. Soc.* **1991**, *74*, 440.
- (36) Hernandez, M. T.; Jurado, J. R.; Duran, P. *J. Am. Ceram. Soc.* **1991**, *74*, 1254.

- (37) Jue, J. F.; Chen, J.; Virkar, A. V. *J. Am. Ceram. Soc.* **1991**, *74*, 1811.
- (38) Sakka, Y. *J. Mater. Sci. Lett.* **1992**, *11*, 18.
- (39) Hirano, M. *Br. Ceram. Trans. J.* **1992**, *91*, 139.
- (40) Kountouros, P.; Petzow, G. In *Science and Technology of Zirconia V*; Badwal, S. P. S., Bannister, M. J., Hannink, R. H. J., Eds.; Technomic: Lancaster, 1993; p 30.
- (41) Drennan, J.; Hartshorn, A. J.; Thompson, S. W. In *Science and Technology of Zirconia V*; Badwal, S. P. S., Bannister, M. J., Hannink, R. H. J., Eds.; Technomic: Lancaster, 1993; p 144.
- (42) Hughes, A. E.; Ciacchi, F. T.; Badwal, S. P. S. In *Science and Technology of Zirconia V*; Badwal, S. P. S., Bannister, M. J., Hannink, R. H. J., Eds.; Technomic: Lancaster, 1993; p 152.
- (43) Kruse, O.; Carstanjen, H. D.; Kountouros, P. W.; Schubert, H.; Petzow, G. In *Science and Technology of Zirconia V*; Badwal, S. P. S., Bannister, M. J., Hannink, R. H. J., Eds.; Technomic: Lancaster, 1993; p 163.
- (44) Azzoni, C. B.; Paleari, A.; Scardina, F.; Krajewski, A.; Ravaglioli, A.; Meschke, F. *J. Mater. Sci.* **1993**, *28*, 3951.
- (45) Kim, Y. S.; Jung, C. H.; Park, J. Y. *J. Nucl. Mater.* **1994**, *209*, 326.
- (46) Hughes, A. E.; Ciacchi, F. T.; Badwal, S. P. S. *J. Mater. Chem.* **1994**, *4*, 257.
- (47) Srikanth, V.; Subbarao, E. C. *J. Mater. Sci.* **1994**, *29*, 3363.
- (48) Zhu, H. Y. *J. Mater. Sci.* **1994**, *29*, 4351.
- (49) Lee, J. K.; Kim, H. *Ceram. Int.* **1994**, *20*, 413.
- (50) Govila, R. K. *J. Mater. Sci.* **1995**, *30*, 2656.
- (51) Lawson, S. *J. Eur. Ceram. Soc.* **1995**, *15*, 485.
- (52) Basu, D.; Dasgupta, A.; Sinha, M. K.; Sartar, B. K. *Ceram. Int.* **1995**, *21*, 277.
- (53) Lofthouse, G. C.; Lawson, S.; Gill, C. *Key Eng. Mater.* **1995**, *99–100*, 265.
- (54) Hughes, A. E.; St John, H.; Kountouros, P.; Schubert, H. *J. Eur. Ceram. Soc.* **1995**, *15*, 1125.
- (55) Yashima, M.; Nagatome, T.; Noma, T.; Ishizawa, N.; Suzuki, Y.; Yoshimura, M. *J. Am. Ceram. Soc.* **1995**, *78*, 2229.
- (56) Boutz, M. M. R.; Winnubst, A. J. A.; van Langerak, B.; Olde Scholtenhuis, R. J. M.; Kreuwel, K.; Burggraaf, A. J. *J. Mater. Sci.* **1995**, *30*, 1854.
- (57) Kim, D. J.; Jung, H. J.; Cho, D. H. *Solid State Ionics* **1995**, *80*, 67.
- (58) Basu, D.; Dasgupta, A.; Basu, M. K.; Sartar, B. K. *J. Eur. Ceram. Soc.* **1996**, *16*, 613.
- (59) Tan, H. C.; Gill, C.; Lawson, S. *Key Eng. Mater.* **1996**, *113*, 199.
- (60) Lawson, S.; Gill, C.; Dransfield, G. P. *Key Eng. Mater.* **1996**, *113*, 207.
- (61) Li, J. F.; Watanabe, R. *Mater. Trans., JIM* **1996**, *37*, 1171.
- (62) Li, J. F.; Watanabe, R.; Zhang, B. P.; Asami, K.; Hashimoto, K. *J. Am. Ceram. Soc.* **1996**, *79*, 3109.
- (63) Li, J. F.; Watanabe, R. *J. Mater. Sci.* **1997**, *32*, 1149.
- (64) Hirano, M.; Kato, E. *J. Ceram. Soc. Jpn.* **1997**, *105*, 37.
- (65) Kim, D. J. *J. Eur. Ceram. Soc.* **1997**, *17*, 897.
- (66) Chung, T. J.; Song, H.; Kim, G. H.; Kim, D. Y. *J. Am. Ceram. Soc.* **1997**, *80*, 2607.
- (67) Bowen, C.; Ramesh, S.; Gill, C.; Lawson, S. *J. Mater. Sci.* **1998**, *33*, 5103.
- (68) Jansen, S. R.; Winnubst, A. J. A.; He, Y. J.; Verweij, H.; van der Varst, P. G. T.; de With, G. *J. Eur. Ceram. Soc.* **1998**, *18*, 557.
- (69) Kim, D. J.; Jung, H. J.; Jang, J. W.; Lee, H. L. *J. Am. Ceram. Soc.* **1998**, *81*, 2309.
- (70) Merle-Mejean, T.; Barberis, P.; Othmane, S. B.; Nardou, F.; Quintard, P. E. *J. Eur. Ceram. Soc.* **1998**, *18*, 1579.
- (71) Li, J. F.; Watanabe, R. *J. Am. Ceram. Soc.* **1998**, *81*, 2687.
- (72) Guo, X. *Solid State Ionics* **1998**, *112*, 113.
- (73) Guo, X. *J. Phys. Chem. Solids* **1999**, *60*, 539.
- (74) Kim, Y. S.; Kwon, S. C. *J. Nucl. Mater.* **1999**, *270*, 165.
- (75) Lee, D. Y.; Kim, D. J.; Jang, J. W.; Choi, D. W.; Lee, S. J. *Mater. Lett.* **1999**, *39*, 221.
- (76) Belous, A. G.; Makarenko, A. N.; Pashkova, E. V.; Khomenko, B. S. *Inorg. Mater.* **1999**, *35*, 1147.
- (77) Wada, S.; Yokoyama, K. *J. Ceram. Soc. Jpn.* **1999**, *107*, 92.
- (78) Ohmichi, N.; Kamioka, K.; Ueda, K.; Matsui, K.; Ohgai, M. *J. Ceram. Soc. Jpn.* **1999**, *107*, 128.
- (79) Ohmichi, N.; Kamioka, K.; Ueda, K.; Matsui, K.; Ohgai, M. *J. Ceram. Soc. Jpn.* **1999**, *107*, 820.
- (80) Hirano, M.; Kato, E. *J. Mater. Sci.* **1999**, *34*, 1399.
- (81) Ramesh, S.; Gill, C.; Lawson, S. *J. Mater. Sci.* **1999**, *34*, 5457.
- (82) Koh, Y. H.; Kong, Y. M.; Kim, S.; Kim, H. E. *J. Am. Ceram. Soc.* **1999**, *82*, 1456.
- (83) Ho, F. Y.; Wei, W. C. J. *J. Am. Ceram. Soc.* **1999**, *82*, 1614.
- (84) Chevalier, J.; Cales, B.; Drouin, J. M. *J. Am. Ceram. Soc.* **1999**, *82*, 2150.
- (85) Zhu, W. Z.; Zhang, X. B. *Scr. Mater.* **1999**, *40*, 1229.
- (86) Guo, X. *Adv. Eng. Mater.* **2000**, *2*, 604.
- (87) Yasuda, K.; Takeda, H. *J. Mater. Sci.* **2000**, *35*, 4379.
- (88) Djurado, E.; Dessemond, L.; Roux, C. *Solid State Ionics* **2000**, *136–137*, 1249.
- (89) Guo, X. *Phys. Status Solidi A* **2000**, *177*, 191.
- (90) Guo, X. *J. Mater. Sci.* **2001**, *36*, 3737.
- (91) Shojai, F.; Mäntylä, T. A. *J. Eur. Ceram. Soc.* **2001**, *21*, 37.
- (92) Shojai, F.; Mäntylä, T. A. *Ceram. Int.* **2001**, *27*, 299.
- (93) Li, J. G.; Zhang, L. M.; Shen, Q.; Hashida, T. *Mater. Sci. Eng. A* **2001**, *297*, 26.
- (94) Cai, S.; Yuan, Q. M.; Meng, J. H.; Yang, Z. F.; Chen, Y. *J. Eur. Ceram. Soc.* **2001**, *21*, 2911.
- (95) Grant, K. L.; Rawlings, R. D.; Sweeney, R. *J. Mater. Sci.-Mater. Med.* **2001**, *12*, 557.
- (96) Yasuda, K.; Goto, Y.; Takeda, H. *J. Am. Ceram. Soc.* **2001**, *84*, 1037.
- (97) Oskarsson, M.; Ahlberg, E.; Pettersson, K. *J. Nucl. Mater.* **2001**, *295*, 126.
- (98) Lance, M. J.; Vogel, E. M.; Reith, L. A.; Cannon, W. R. *J. Am. Ceram. Soc.* **2001**, *84*, 2731.
- (99) Guo, R.; Guo, D.; Zhao, D.; Yang, Z.; Chen, Y. *Mater. Lett.* **2002**, *56*, 1014.
- (100) Kanellopoulos, P.; Gill, C. *J. Mater. Sci.* **2002**, *37*, 5075.
- (101) Lin, J. D.; Duh, J. G.; Lo, C. L. *Mater. Chem. Phys.* **2002**, *77*, 808.
- (102) Munoz-Saldana, J.; Balmori-Ramirez, H.; Jaramillo-Vigueras, D.; Iga, T.; Schneider, G. A. *J. Mater. Res.* **2003**, *18*, 2415.
- (103) Menezes, C. A. B.; Lazar, D. R. R.; Ussui, V.; Lima, N. B.; Paschoal, J. O. A. *Mater. Sci. Forum* **2003**, *416*, 573.
- (104) Roebben, G.; Basu, B.; Vleugels, J.; van der Biest, O. *J. Eur. Ceram. Soc.* **2003**, *23*, 481.
- (105) Zhao, Z. B.; Liu, C.; Northwood, D. O. *Key Eng. Mater.* **2003**, *233–236*, 655.
- (106) Kim, D. J.; Lee, D. Y.; Han, J. S. *Key Eng. Mater.* **2003**, *240–242*, 831.
- (107) Guo, X.; He, J. *Acta Mater.* **2003**, *51*, 5123.
- (108) Boulch, F.; Dessemond, L.; Djurado, E. *J. Eur. Ceram. Soc.* **2004**, *24*, 1181.
- (109) Guo, X.; Schober, T. *J. Am. Ceram. Soc.* **2004**, *87*, 746.
- (110) Djurado, E.; Boulch, F.; Dessemond, L.; Rosman, N.; Mermoux, M. *J. Electrochem. Soc.* **2004**, *151*, A774.
- (111) Livage, J.; Doi, K.; Mazieres, C. *J. Am. Ceram. Soc.* **1968**, *51*, 349.
- (112) Fabris, St.; Paxton, A. T.; Finnis, M. W. *Acta Mater.* **2002**, *50*, 5171.
- (113) Kreuer, K. D. *Chem. Mater.* **1996**, *8*, 610.
- (114) Kreuer, K. D. *Solid State Ionics* **1999**, *125*, 285.
- (115) Kreuer, K. D.; Adams, St.; Münch, W.; Fuchs, A.; Klock, U.; Maier, J. *Solid State Ionics* **2001**, *145*, 295.
- (116) Redfern, S. E.; Grimes, R. W.; Rawlings, R. D. *J. Mater. Chem.* **2001**, *11*, 449.
- (117) Simpson, L. A.; Carter, R. E. *J. Am. Ceram. Soc.* **1966**, *49*, 139.
- (118) Norby, T. In *Advances in Zirconia Science and Technology*; Meriani, S., Palmonari, C., Eds.; Elsevier: New York, 1989; p 209.
- (119) Raz, S.; Sasaki, K.; Maier, J.; Riess, I. *Solid State Ionics* **2001**, *143*, 181.
- (120) Guo, X. *Solid State Ionics* **1995**, *81*, 235.
- (121) Guo, X.; Maier, J. *J. Electrochem. Soc.* **2001**, *148*, E121.
- (122) Guo, X.; Sigle, W.; Fleig, J.; Maier, J. *Solid State Ionics* **2002**, *154–155*, 555.
- (123) Guo, X. *Comput. Mater. Sci.* **2001**, *20*, 168.
- (124) Guo, X.; Zhang, Z. *Acta Mater.* **2003**, *51*, 2539.
- (125) Etsell, T. H.; Flengas, S. N. *Chem. Rev.* **1970**, *70*, 339.
- (126) Mackrodt, W. C.; Woodrow, P. M. *J. Am. Ceram. Soc.* **1986**, *69*, 277.
- (127) Behrens, G.; Heuer, A. H. *J. Am. Ceram. Soc.* **1996**, *79*, 895.

CM040167H